

Claremont Colleges

Scholarship @ Claremont

HMC Senior Theses

HMC Student Scholarship

2022

An Adaptive Hegselmann–Krause Model of Opinion Dynamics

Phousawanh Peaungvongpakdy

Follow this and additional works at: https://scholarship.claremont.edu/hmc_theses



Part of the [Dynamic Systems Commons](#), and the [Non-linear Dynamics Commons](#)

Recommended Citation

Peaungvongpakdy, Phousawanh, "An Adaptive Hegselmann–Krause Model of Opinion Dynamics" (2022).
HMC Senior Theses. 262.

https://scholarship.claremont.edu/hmc_theses/262

This Open Access Senior Thesis is brought to you for free and open access by the HMC Student Scholarship at Scholarship @ Claremont. It has been accepted for inclusion in HMC Senior Theses by an authorized administrator of Scholarship @ Claremont. For more information, please contact scholarship@claremont.edu.

An Adaptive Hegselmann–Krause Model of Opinion Dynamics

Phousawanh Peaungvongpakdy

Heather Zinn-Brooks, Advisor

Andrew Bernoff, Reader



Department of Mathematics

May, 2022

Copyright © 2022 Phousawanh Peaungvongpakdy.

The author grants Harvey Mudd College and the Claremont Colleges Library the nonexclusive right to make this work available for noncommercial, educational purposes, provided that this copyright statement appears on the reproduced materials and notice is given that the copying is by permission of the author. To disseminate otherwise or to republish requires written permission from the author.

Abstract

Models of opinion dynamics have been used to understand how the spread of information in a population evolves, such as the classical Hegselmann–Krause model (Hegselmann and Krause, 2002). One extension of the model has been used to study the impact of media ideology on social media networks (Brooks and Porter, 2020). In this thesis, we explore various models of opinions and propose our own model, which is an adaptive version of the Hegselmann–Krause model. The adaptive version implements the social phenomenon of *homophily*—the tendency for like-minded agents to associate together. This is done by having agents dissolve connections if their opinions are too different from one another and establish new connections probabilistically, with it being more likely to establish a connection with an agent with a similar opinion to theirs. We study how our model changes with various values of the parameters in the model, namely the confidence parameter and homophily parameter, as well as different initial graph topologies and varying the number of nodes in the graph.

Contents

Abstract	iii
Acknowledgments	xi
1 Duties to Democracy	1
2 Background Information: Various Models of Opinion Dynamics	5
2.1 French–Degroot Model	5
2.2 The Hegselmann–Krause Model	6
2.3 Deffaunt–Weisbuch Model	8
2.4 An Adaptive Deffaunt–Weisbuch Model	10
3 The Adaptive HK Model	15
3.1 The Adaptive HK Model	15
3.2 Components in the graph & the graph Laplacian	18
3.3 The Difference Metric	22
3.4 Scalar Assortativity Coefficient	24
4 Results of the Adaptive HK Model	27
4.1 Analyzing the HK model	27
4.2 Graph topologies of interest	27
4.3 Update, then rewire	29
4.4 Rewire, then update	34
4.5 Varying the number of nodes	39
4.6 Varying p in the Erdős–Rényi model	41
5 Conclusion & Future Work	45
5.1 Conclusion	45
5.2 Future Work	46

Bibliography

49

List of Figures

2.1	An example of the French–Degroot model of opinion dynamics. The characters in this model are asked their opinions of acorns, where an opinion of 0 represents absolute disgust with acorns and an opinion of 1 represents utter infatuation with acorns. Any opinion in between 0 and 1 will represent a combination of these views. In 2.1a we randomly assign each character an opinion and have arrows representing the interactions they have with each other. In 2.1b we display one node’s opinion update with the Hans the hedgehog. 2.1c gives what the new opinions are for all characters for the first timestep.	7
2.2	In this example we use the same network as in 2.1. Here we let $C = 0.2$ and we observe that only one node pair and influences each other’s opinions.	9
2.3	An example of the adaptive DW model. The initial graph topologies and opinions are the same as 2.1a. In 2.3a we have the the discordant set defined with $\beta = .3$ and it was chosen randomly that the connection with the squirrel and hedgehog character that their connection would be dissolved. In 2.4a we establish a new connection with the squirrel and penguin character.	12
2.4	An example of the adaptive DW model. The initial graph topologies and opinions are the same as 2.1a. In 2.3a we have the the discordant set defined with $\beta = .3$ and it was chosen randomly that the connection with the squirrel and hedgehog character that their connection would be dissolved. In 2.4a we establish a new connection with the squirrel and penguin character.	12

3.1	The converged model for $C = 0.1$ and $\beta = 0.1$ for 3.1a and $C = 0.1$ and $\beta = 0.3$ for 3.1b. Observe that the number of components would be calculated to be 1 in either case but the distribution of opinions varies widely. Notice though that if we were to use the difference metric that $d < 1$ for 3.1a while $d = 1$ for 3.1b.	22
4.1	Convergence times for the various graph topologies for $n = 100$. The deepest shade of blue represents the fastest convergence time of $t = 2$ while the yellow represents the slowest convergence time of $t = 7$	30
4.2	Number of components for the various graph topologies for $n = 100$. The deepest shade of blue represents the smallest number of components of $c = 1$ while the yellow represents the largest number of components of $c \approx 2$	30
4.3	The difference metric for various graph topologies for $n = 100$. The deepest shade of blue represents the smallest difference metric value of $d = 0.1$ while the yellow represents the largest value of $d = 1$	30
4.4	The scalar assortativity coefficient for $n = 100$. The deepest shade of blue represents the smallest scalar assortativity coefficient of $r = 0$ while the yellow represents the largest coefficient value of $r = 1$	30
4.5	Convergence times for the various graph topologies for $n = 100$. The deepest shade of blue represents the fastest convergence time of $t = 2$ while the yellow represents the slowest convergence time of $t = 6$	35
4.6	Number of components for the various graph topologies for $n = 100$. The deepest shade of blue represents the smallest number of components of $c = 1$ while the yellow represents the largest number of components of $c \approx 2.2$	35
4.7	The difference metric for various graph topologies for $n = 100$. The deepest shade of blue represents the smallest difference metric value of $d = 0.1$ while the yellow represents the largest value of $d = 1$	35
4.8	The scalar assortativity coefficient for $n = 100$. The deepest shade of blue represents the smallest scalar assortativity coefficient of $r = 0$ while the yellow represents the largest coefficient value of $r = 1$	35

4.9	Summary statistics for “Update, then rewire” version on $G(n, p = 0.6)$ for various values of n	40
4.10	Summary statistics for “Rewire, then update” version on $G(n, p = 0.6)$ for various values of n	40
4.11	Summary statistics for “Update, then rewire” version on $G(n = 100, p)$ for various values of p	42
4.12	Summary statistics for “Rewire, then update” version on $G(n = 100, p)$ for various values of p	42

Acknowledgments

One of the premises of this thesis is that opinions of people are reflected through relationships with others. The same is true for this thesis itself. I am grateful for those who have shaped, guided, and encouraged not only the thoughts and writing of this thesis but my own mathematical development. I would like to thank my thesis advisor, Heather Zinn-Brooks, for her guidance and invaluable advice not only pertaining to math but life in general. Prof. Heather, thank you not only for pushing my mathematical knowledge and listening to my ideas but also for all the tea, banana bread, and snacks you provided during our meetings. I would also like to thank Darryl Yong, whose guidance and mentorship has helped shape the ongoing adventure for fulfillment and myself. Prof. Yong, it was because of your social justice class that I take into heart HMC's mission statement in everything I do, including this thesis—and I am eternally grateful for it. Also, thanks for all the anime recommendations and the food, hehe. Furthermore, I would like to thank the thesis advisor Jon Jacobsen for his guidance in this process. Prof. Jakes, I am grateful for the life advice you gave me during my frosh year and during thesis. I am also grateful for Andrew Bernoff, not only for being my second reader but also relighting my passion for applied mathematics during my senior year. Prof. Bernoff, your course in partial differential equations reminded me what I love about applied math and I am thankful for that. Finally, I would also like to thank the HMC Mathematics department, especially DruAnn Thomas and Melissa Hernandez-Alvarez for their support in writing this thesis—thank you for all the candy!

I would also like to thank my Summer 2021 research group for their support as well, in particular, special thanks to Solomon Caplan-Valore and Christina Catlett. It was during this time that most of the ideas of this thesis were developed into what it was today.

Finally, I would also like to thank my friends for their support not only throughout my senior year but also through my time at HMC. I am only

who I am today through the support of my friends. They know who they are.

Chapter 1

Duties to Democracy

“As citizens of this democracy,
you are the rulers and the ruled,
the lawgivers and the
law-abiding, the beginning and
the end”

— Adlai Stevenson

We open this thesis with the debate Walter Lippman and John Dewey had pertaining to democracy and people’s obligations to democracy. Starting in 1922, Lippman and Dewey argued back and forth what the impact of public opinion and the obligations people have to democracy (Whipple, 2005). Lippman was fearful of the role that media had to play and feared that the mixture of media and human bias would result in a “pseudo-environment” where people only confirm their own biases and championed the democratic process of only the select elite in his book *Public Opinion* (1922). Dewey, on the other hand, welcomed the ambiguity of knowledge but placed a greater emphasis on everyday people’s obligations to contribute to democracy not only as a realization of community but as an ethical obligation of all in his book *The Public and its Problems* (1927). Whether one takes a Lippmannian or Deweyian perspective on democracy, their debate brings to light to the danger democracy is in due to media.

Scholars have debated on how social media has been used as a tool for “information welfare” which may have contributed to democracy decay in various states (Sloss, 2020). Scholars have also noted that through social media platforms that false information and propaganda are often shared to

reinforce previous biases (Cinelli et al., 2020). The idea of information spread is not new, as there has been previous work to examine the spread of content of media through the viewpoint as disease spread with compartmental models, as studied in (Wang et al., 2014) and (Liu et al., 2017). Another thing that we also consider is the manifestation of “echo chambers” (Flaxman et al., 2016) on social media, where scholars typically define these environments where individuals primarily interact with like-minded individuals. Some scholars have argued these echo chambers have been caused by the spread of misinformation in social media networks and online platforms particularly (Flaxman et al., 2016), (Del Vicario et al., 2016), and some have proposed models for echo chambers in social media (Baumann et al., 2020). These social media networks, such as Twitter, Facebook, and Instagram, have a graph-like structure from people following and being followed by others. These networks can be modeled as a graph and provides a possibility in which we may study the spread of information in social media networks.

Scholars believe the study of polarization to be of importance because of its threat to U.S. democracy. Mann and Ornstein argue this in their book (2012) and claims that polarization’s threat to U.S. democracy is due to the dysfunction between the political parties. Some of the consequences includes the rise of obstructionist tactics and abandonment of compromise between the two parties. Because of obstructionist tactics and lack of compromise between the political parties in the U.S., a deadlock in Congress has occurred, effectively stalling progress and policy-making that could help alleviate inequalities. Since there has been evidence suggesting that misinformation causes polarization, my hope is that by studying misinformation in social media networks, we may better understand the characteristics that allow polarization to occur.

Various models of opinion dynamics have been proposed to understand the spread of misinformation, such as the compartmental models mentioned before (Wang et al., 2014) (Liu et al., 2017) and one through a network perspective (Brooks and Porter, 2020)¹. One way that we can further extend this work is to consider the social phenomenon of homophily, which sociologists have defined to be the tendency for people to associate with other like minded people (McPherson et al., 2001). Here we incorporate the idea of homophily to the Hegselmann–Krause model of opinion dynamics. It is difficult to study these models analytically and one thing that has been

¹I do not mean to imply that this is the only network model that has studied the spread of misinformation.

done in the past is study the effect of initial topologies of the graphs , which has been examined for the Deffaunt–Weisbuch model(Meng et al., 2018). Here we take inspiration and investigate how the initial topology of the graph affects the "components" or manifestation of community structure when our model is at convergence.

The structure of the thesis will be as follows. First we will explore some basic models of opinion dynamics, done in Chapter 2. From there, we present the rules of the adaptive Hegselmann–Krause model in Chapter 3. After introducing the model, we give the summary statistics in which we evaluate the model, the results of the model, and the analysis itself in Chapter 4. Finally, give the recap of the findings in the conclusion and we comment on possible future work in Chapter 5.

Chapter 2

Background Information: Various Models of Opinion Dynamics

"Happiness is promoted by associations of persons with similar tastes and similar opinions"

— Bertrand Russell

2.1 French–Degroot Model

Our first model of opinion dynamics will be one averaging the opinions of agents in a population, also known as the **French–Degroot Model** (Degroot, 1974). Let $G(V, E)$ be a graph with the vertex set V and edge set E . V represents the N people in the population and E encodes the interactions of the people in the population. That is, if two people interact with each other, then there will be an edge between them. We associate an opinion to each person (i.e., each node). We do this by assigning a value $x_i \in [0, 1]$ which represents the opinion of node i . This value can be construed to measure one's political ideology—e.g., 0 may represent a person having the most liberal ideology, 1 may represent a person having the most conservative ideology and any value in between represents a mix of both ideologies.

Each node's opinion updates over time based on the interactions with surrounding nodes. One way we can encode the interactions to update the opinions is through the French–Degroot model, as this is one way to model consensus-seeking behavior. For some node's opinion x_i we say its new updated opinion may be represented as

$$x_i^{t+1} = x_i^t + \frac{1}{I(i) + 1} \sum_{n=1}^N x_j^t \quad (2.1)$$

where $I(i)$ represents the number of neighbors node i has.

This averaged opinion model can be also understood as a heat equation projected onto the graph. These models and their behavior are well understood. Their behavior is beyond the scope of this paper but one may refer to the following resources for their behavior (Lawler, 2010). We include an example in Figure 2.1.¹

2.2 The Hegselmann–Krause Model

One development of the model above was proposed by Rainer Hegselmann and Ulrich Krauss (see 2002 and 2015). In this model, Hegselmann and Krause sought to incorporate complexities in how opinions are shared. In particular, they incorporate the notion of selective exposure, which is the idea is that one only want to incorporate ideas that are "close" to you or opinions that align closely with your opinion. This reflects a lack of willingness of individuals to incorporate opinions that are widely dissonant from their own.

This idea of being selective in incorporating one's opinion to their has developed into a model known as the **bounded-confidence** model. The idea of "closeness" for opinions may be represented through a metric.² Let the opinions be the same as in the repeated opinion averaging model, that is $x_i \in [0, 1]$. Then one sufficient metric in measuring the difference of opinions can be through

$$d(x_i, x_j) = |x_i - x_j|.$$

¹In the examples that follows, characters will be used to represent the agents. The characters are: Hans the hedgehog, Tera the penguin, Pudgy the pug, Cat the cat, and Mudd Squirrel the squirrel. No feelings were hurt in the production of this thesis.

²Usually these metrics satisfy the conditions that define metric spaces in Real Analysis.

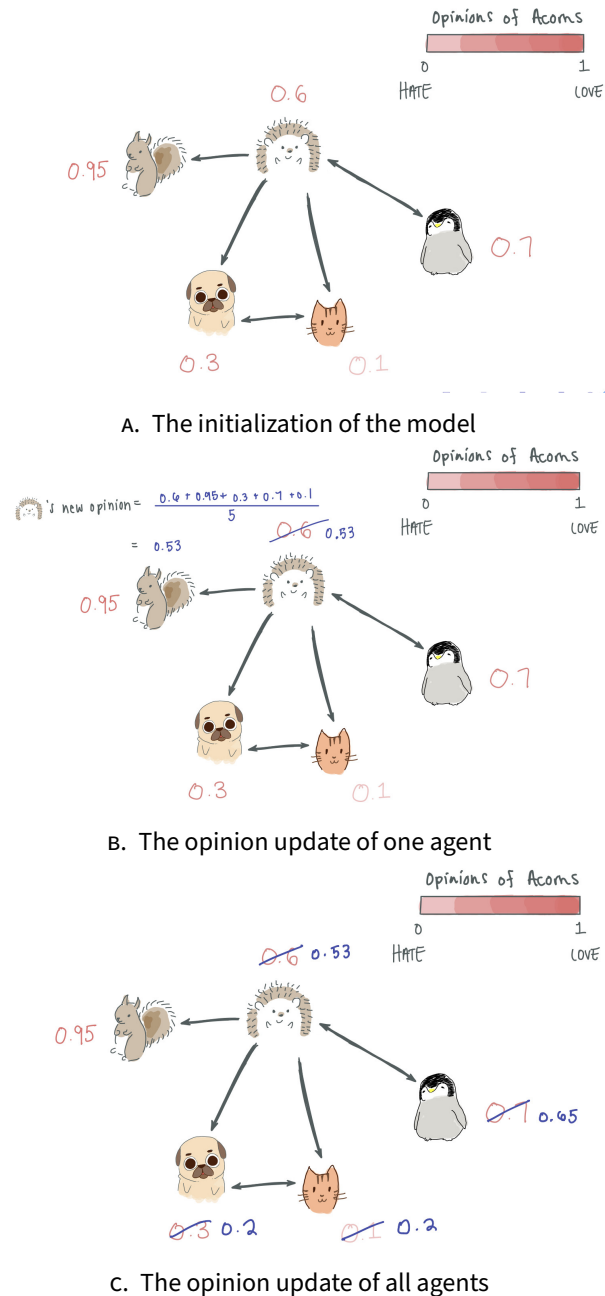


FIGURE 2.1 An example of the French–Degroot model of opinion dynamics. The characters in this model are asked their opinions of acorns, where an opinion of 0 represents absolute disgust with acorns and an opinion of 1 represents utter infatuation with acorns. Any opinion in between 0 and 1 will represent a combination of these views. In 2.1a we randomly assign each character an opinion and have arrows representing the interactions they have with each other. In 2.1b we display one node’s opinion update with the Hans the hedgehog. 2.1c gives what the new opinions are for all characters for the first timestep.

With this metric defined, we modify the opinion update rule of the French–Degroot model by having the opinion update rule for node i node to be given by

$$x_i^{t+1} = x_i^t + \frac{1}{I(i) + 1} \sum_{n=1}^N x_j^t \cdot f(x_i^t, x_j^t) \quad (2.2)$$

where f is an indicator function given by

$$f(x_i, x_j) = \begin{cases} 1 & \text{if } |x_i - x_j| \leq C \\ 0 & \text{otherwise.} \end{cases}$$

Here C is called the **confidence parameter**. This parameter controls how receptive an agent is to an opinion. For large values of C , agents are more likely have a higher tolerance of taking in different opinions than theirs while low values of C will have agents be less receptive to different opinions than theirs. This new opinion update, in Equation 2.2, gives us our first bounded-confidence model of opinion dynamics, which is called the **Hegselmann–Krause (HK)** model. One noteworthy thing we would like to point out is this model of opinion dynamics has agents update their opinions *synchronously*—that is, all the agents update their opinions at the same time. While this seems like a benign feature, our next model shows that this feature can lead to different quantitative results of other models of opinion dynamics. In particular, one model of opinion dynamics that has opinions update asynchronously is called the Deffaut–Weisbuch model, which is a stochastic process. Furthermore, the HK model not only incorporates the idea of selective exposure but also consensus-seeking. The French–Degroot model only considers consensus-seeking behavior.

We consider another example given in Figure 2.2. Consider the same network as given in 2.1. Let us set the confidence parameter to be $C = 0.2$. We note that only one pair of agents exchange opinions as their difference is $0.1 < C = 0.2$. For all other agents in the graph, we do not update opinions. With this bounded-confidence rule, we can already see that the end behavior is different from the French-Degroot model after many time steps.

2.3 Deffaut–Weisbuch Model

In the **Deffaut–Weisbuch (DW)** model, randomly-selected neighboring agents interact in a pairwise manner and make a compromise toward each

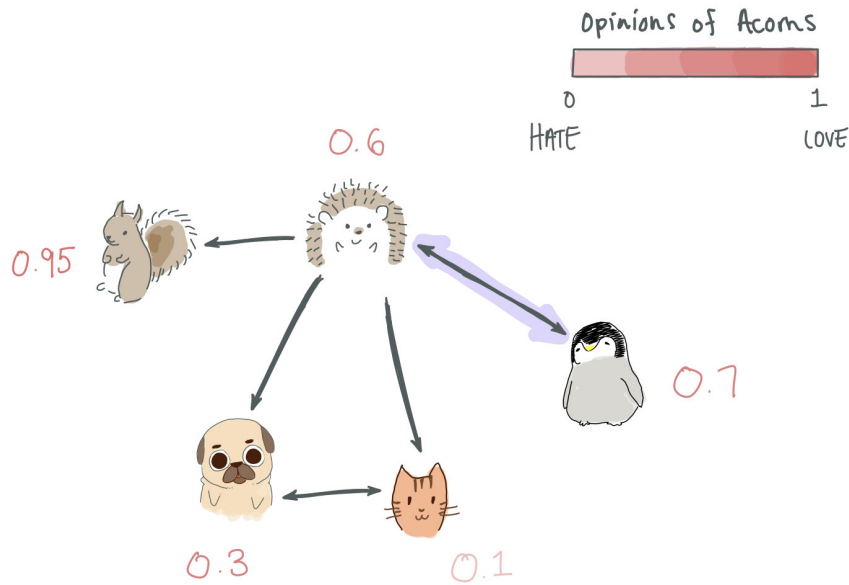


FIGURE 2.2 In this example we use the same network as in 2.1. Here we let $C = 0.2$ and we observe that only one node pair and influences each other's opinions.

other's opinion whenever their opinion difference is below a given threshold. Consider a population of N agents, who are connected to each other socially via a network $G(V, E)$ with vertex set V and edge set E . Let $[0, 1]$ be the opinion space. At time t , suppose that each agent i holds a time-dependent opinion $x_i(t) \in [0, 1]$. Given an initial profile $\vec{x}(0) \in [0, 1]^N$, a confidence bound $C \in [0, 1]$, and a cautiousness parameter that we call the multiplier $m \in (0, 0.5]$, the Deffaunt–Weisbuch model is the random process defined as follows: at time t , a pair of neighboring agents i and $j \neq i$ are selected uniformly at random and updated according to the equations

$$x_i(t+1) = \begin{cases} x_i(t) + m\Delta_{j,i}(t) & \text{if } |\Delta_{i,j}(t)| < C, \\ x_i(t) & \text{otherwise,} \end{cases} \quad (2.3)$$

$$x_j(t+1) = \begin{cases} x_j(t) + m\Delta_{i,j}(t) & \text{if } |\Delta_{j,i}(t)| < C, \\ x_j(t) & \text{otherwise,} \end{cases} \quad (2.4)$$

where $\Delta_{j,i}(t) = x_j(t) - x_i(t)$.

One thing that we would like to stress that this model has agents update their opinions in a pairwise manner, which is not the same as

updating opinions synchronously. Work has been done to explore the model quantitatively through simulations (2018).

2.4 An Adaptive Deffaunt–Weisbuch Model

One thing that has not been considered in these models of opinion dynamics is the fact that connections among agents may not stay static. Agents often form new connections as well as dissolve connections with other agents. This phenomenon is called *homophily*, or the tendency for like-minded agents to form connections with other like-minded agents (2001). Unchitta Kan, Mason A. Porter, and Michelle Feng implemented this idea of homophily to the Deffaunt–Weisbuch model as an adaptive model and we discuss their work below Kan et al. (2021).

Let $G(V, E)$ be a undirected graph. Let the opinion space be $[0, 1]$ and let each agent i have an opinion $x_i \in [0, 1]$. Let us define the **discordant edge set** to be $E_d^\beta = \{(i, j) \in E : |x_i - x_j| > \beta\}$ where we call β the **homophily parameter**. At each time step, two processes occur in sequence:

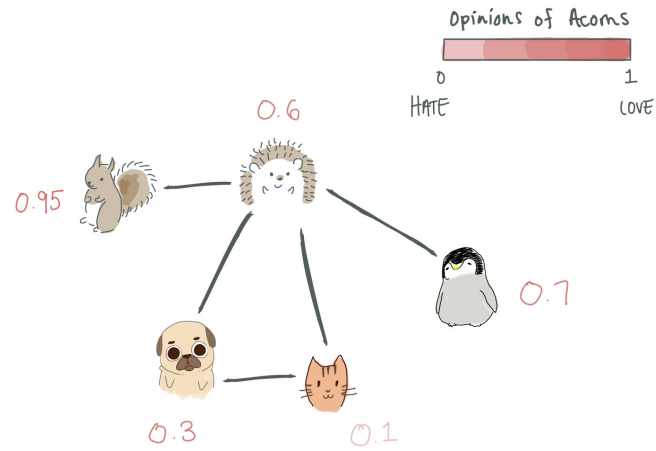
1. M discordant edges are chosen uniformly at random to rewire—this is called the **rewiring rule**.
2. K edges are chosen uniformly at random to interact based off the opinion update rules of DW in Equation 2.3 and Equation 2.4—this is called the **opinion update rule**.

The **rewiring** is as follows:

1. M edges are selected uniformly at random from E_d^β .
2. Each edge (i, j) is dissolved, and either i or j is selected with randomly from a uniform distribution to rewire to another node k .
3. k is chosen from the probability distribution $P(i \rightarrow k) \propto (1 - d(x_i, x_k))$ where $d(x_i, x_k) = |x_i - x_k|$.
4. Edges (i, k) or (j, k) is added to E^{t+1} and $E_d^\beta(t + 1)$ if it discordant.

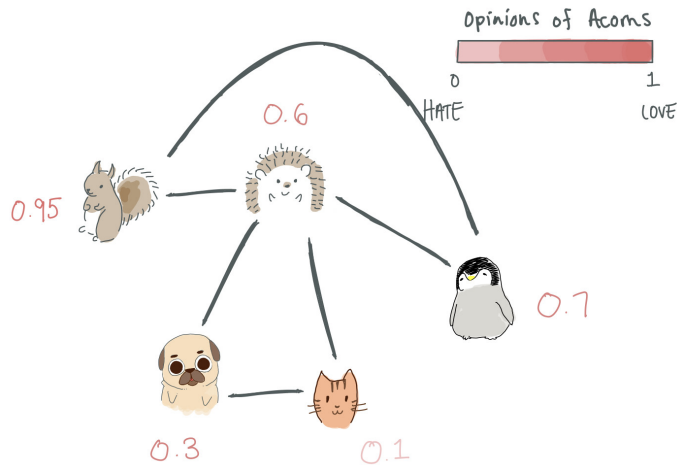
Afterwards, the model follows the **opinion update rules** of the classical Deffaunt–Weisbuch model given by (2.3) and (2.4). An example is given in Figure 2.3. In their explorations of the model, they found that the initial graph topology and the homophily parameter β played a big role in the

convergence time of the model and community formation. In particular, low values of C and β resulted in a large number of clusters while convergence time was greatest for low values of C and β . For more detail on the work, see Kan et al. (2021).



A. The DW model dissolving the connection

FIGURE 2.3 An example of the adaptive DW model. The initial graph topologies and opinions are the same as 2.1a. In 2.3a we have the the discordant set defined with $\beta = .3$ and it was chosen randomly that the connection with the squirrel and hedgehog character that their connection would be dissolved. In 2.4a we establish a new connection with the squirrel and penguin character.



A. The DW model reestablishing a new connection

FIGURE 2.4 An example of the adaptive DW model. The initial graph topologies and opinions are the same as 2.1a. In 2.3a we have the the discordant set defined with $\beta = .3$ and it was chosen randomly that the connection with the squirrel and hedgehog character that their connection would be dissolved. In 2.4a we establish a new connection with the squirrel and penguin character.

Inspired by Kan et al.'s work on the adaptive Deffaunt–Weisbuch model, we seek to develop and analyze an adaptive version of the synchronously-updating Hegselmann–Krause model. We discuss our model in the next chapter.

Chapter 3

The Adaptive HK Model

In this chapter we provide our work in developing an adaptive Hegselmann–Krause model of opinion dynamics. Our work was heavily influenced by Kan et al. (2021) in developing an adaptive DW model. In this section we give the model and summary statistics used to evaluate the model.

3.1 The Adaptive HK Model

Let $G(V, E)$ be our graph with the vertex set V and edge set E . Let $|V| = N$ and let C and β be the confidence bound parameter and homophily parameter as we described in (2.2) and (2.4) respectively. Furthermore, we randomly assign each vertex i an opinion as done in (2.1). Our model first begins by considering all vertices in the graph. A vertex i has a chance to form an edge with vertex k , where this probability is given by

$$P(i \rightarrow k) = 1 - |x_i - x_k|. \quad (3.1)$$

We call the step above the **rewire step**. After considering all rewires, each vertex i then dissolves a connection with a neighboring vertex j if

$$|x_i - x_j| > \beta. \quad (3.2)$$

Finally, the next opinion at time step $t + 1$ is given by (2.2). We note that we propose two different types of update rules: (1) updating opinions first, then rewiring and (2) rewiring first, then updating opinions. See Algorithm 1 and Algorithm 2—which correlate to the corresponding update rules—to see the overview for each update model.

We provide two update different update rules for two reasons:

1. We initially formulated the model rewiring first then updating first because it was more convenient to code in MATLAB. We noted, however, that this ordering was different from the adaptive Deffaunt-Weisbuch model (Kan et al., 2021)—namely they updated first then rewired. We wanted to see if there were any differences for the sake of it. However, early simulations led us to surprising results, leading to the second reason, namely that
2. We discovered our model was sensitive to updating or rewiring first and we wanted to discover if any conditions changed these results and document where these differences appeared.

We thus explore these two different type of update rules in this work.

For any simulation of updating, a criteria for convergence needs to be given, barring any outstanding circumstances.¹ We would like our model to converge (or rather say agents have reached an opinion consensus of sorts) and thus we say that our model has converged if for all nodes in the graph the change in opinions between two time steps $|x_i^t - x_i^{t+1}| < 10^{-4}$ and no edges were dissolved nor established between the two time steps. The **convergence time** of the model is the number of iterations the model takes to converge per the rules above. We had a bailout time of $t = 500$, that is, we halt the model if the model did not converge after 500 time steps. We picked the bailout time to be $t = 500$ because early simulations of the model resulted in convergence times of around 20 iterations.²

When the model has converged, there needs to be a way to analyze the end results. There are various ways one can do so but we decide to do so with *summary statistics*. They are

1. the convergence time
2. the number of “components”
3. the “difference” metric and
4. the scalar assortativity coefficient.

¹For example, some models do not want a convergence criteria exactly because they would like to run forever.

²The choice of $t = 500$ is going overboard but the author thought it would be better safe than sorry in case there would be any simulation information could be missed or any anomalies.

Algorithm 1 UPDATE, THEN REWIRE

Initialize graph topology
Randomly assign each node x_i an opinion from $[0, 1]$
while model has not converged OR bailout time not exceeded **do**
 for all vertices i **do**
 if $|x_i - x_j| \leq C$ **then**
 Update opinions via average (HK rule)
 end if
 if $|x_i - x_j| > \beta$ **then**
 Dissolve the edge between vertex i and vertex j
 end if
 Add edge from vertex i to vertex k with $P(i \rightarrow k) = 1 - |x_i - x_k|$
 end for
end while

Algorithm 2 REWIRE, THEN UPDATE

Initialize graph topology
Randomly assign each node x_i an opinion from $[0, 1]$
while model has not converged OR bailout time not exceeded **do**
 for all vertices i **do**
 if $|x_i - x_j| > \beta$ **then**
 Dissolve the edge between vertex i and vertex j
 end if
 Add edge from vertex i to vertex k with $P(i \rightarrow k) = 1 - |x_i - x_k|$
 if $|x_i - x_j| \leq C$ **then**
 Update opinions via average (HK rule)
 end if
 end for
end while

The convergence time is the simplest statistic out of the four, giving us the number of time steps in which the convergence criteria was met. We explain what the other three statistics are in greater detail and the interpretation.

3.2 Components in the graph & the graph Laplacian

Because of the evolving edges, we hypothesize that converged models will have disjoint subgraphs that may manifest. These disjoint subgraphs will be called the **components** of the graph. However, this begs the question in how can study the number of components of a graph. Surprisingly, we can do this through the study of zero eigenvectors of the **graph Laplacian**. In this section, we give the background in how the number of components of a graph is related to the graph Laplacian.

Let G be a graph and let A be the adjacency matrix of G and let D be a diagonal matrix with the degree of node i at entry D_{ii} . Then we define the **graph Laplacian** to be

$$L = D - A, \tag{3.3}$$

where the elements of L are given by

$$L_{i,j} = \begin{cases} \kappa_i & \text{if } i = j \\ -1 & \text{if } i \neq j \text{ and } v_i \text{ is adjacent to } v_j \\ 0 & \text{otherwise,} \end{cases} \tag{3.4}$$

where $\kappa_i = \deg(v_i)$.

Another useful definition of the Laplacian is also given by

$$L_{ij} = \kappa_i \delta_{ij} - A_{ij} \tag{3.5}$$

where δ_{ij} is the Kronecker delta and A_{ij} is the entry of the adjacency matrix.

We derive the property that the number of zero eigenvalues of the graph Laplacian is equal to number of components of a graph in the series of lemmas below.

Lemma 3.2.1. *The rows of the Laplacian sum to zero.*

Proof. The elements of each row of the Laplacian is given by (3.4). For any row i , -1 appears κ_i times because the adjacency matrix must have the κ_i 1's in each row by definition. Thus taking the sum of the elements of any row yields $\kappa_i - \kappa_i = 0$. \square

Lemma 3.2.2. *L is real and symmetric.*

Proof. Since L is the sum of a diagonal matrix and an adjacency matrix, L is real and symmetric by construction. \square

Lemma 3.2.3. *The eigenvalues of L are real and nonnegative.*

Proof. From (3.2.2) since we know that L is real and symmetric, this implies that the eigenvalues of L must be real. Thus all that is left to show is that the eigenvalues are nonnegative.

Let v be the eigenvalue of L such that v is normalized—that is $v^\top v = 1$. Observe that by definition of the eigenvalue, we have

$$Lv = \lambda v.$$

Left multiplying both sides by v^\top yields

$$v^\top Lv = v^\top \lambda v \tag{3.6}$$

$$= \lambda. \tag{3.7}$$

The goal of this proof is to show that the left hand side of (3.6) is nonnegative and thus λ is consequently nonnegative as well.

Using the definition of (3.5) we may expand (3.6) to be

$$v^\top Lv = \sum_i \sum_j L_{ij} v_i v_j. \tag{3.8}$$

Substituting the definition of L given by (3.5) we get

$$\sum_i \sum_j L_{ij} v_i v_j = \sum_i \sum_j (\kappa_i \delta_{ij} - A_{ij}) v_i v_j. \tag{3.9}$$

Summing across all j 's, we note that we only get a contribution from the Kronecker delta when $j = i$. This simplifies our sum to be

$$\sum_i \sum_j (\kappa_i \delta_{ij} - A_{ij}) v_i v_j = \sum_i \kappa_i v_i^2 - \sum_i \sum_j A_{ij} v_i v_j.$$

We suspect that we would like to factor in the near future, so we split the first term in half, write the sum indexed with j , and rewrite the sum as

$$\sum_i \kappa_i v_i^2 - \sum_i \sum_j A_{ij} v_i v_j = \frac{1}{2} \sum_i \kappa_i v_i^2 - \sum_i \sum_j A_{ij} v_i v_j + \frac{1}{2} \sum_j \kappa_j v_j^2.$$

Recall from (3.2.1) that the sums of any row equals 0 and that it was a direct consequence because the sum of all the elements of all A must equal κ_i . We use this fact and substitute κ_i with A_{ij} terms so that we have

$$\frac{1}{2} \sum_i \sum_j A_{ij} v_i^2 - \sum_i \sum_j A_{ij} v_i v_j + \frac{1}{2} \sum_j \sum_i A_{ji} v_j^2.$$

We factor out $\frac{1}{2}$ and observe that because $A_{ij} = A_{ji}$ we may rewrite the sum to be

$$\frac{1}{2} \sum_i \sum_j A_{ij} v_i^2 - 2A_{ij} v_i v_j + A_{ij} v_j^2.$$

Consequently, this may be factored as

$$\frac{1}{2} \sum_i \sum_j A_{ij} (v_i - v_j)^2. \quad (3.10)$$

We observe that $A_{ij} \geq 0$ since A only has entries of 1's and 0's and that $(v_i - v_j)^2 \geq 0$ as well. Thus we see that

$$\lambda = \frac{1}{2} \sum_i \sum_j A_{ij} (v_i - v_j)^2 \geq 0$$

which proves that eigenvalues of the Laplacian are nonnegative. \square

Lemma 3.2.4. *L always has at least one zero eigenvalue.*

Proof. From (3.2.1) we know that

$$\sum_j L_{ij} = 0. \quad (3.11)$$

Define $\mathbb{1} = (1, \dots, 1)$. Then (3.11) implies that

$$L\mathbb{1} = 0 \quad (3.12)$$

or that L has an eigenvector $\mathbb{1}$ which corresponds to a 0 eigenvalue. \square

Lemma 3.2.5. *L is not invertible.*

Proof. This follows directly from Lemma 3.2.4. \square

This finally leads us to the major result:

Theorem 3.2.6. *L has c zero eigenvectors if and only if the corresponding graph has c components.*

Proof. First, let us assume that we have a graph with c components. Enumerate each component to have sizes n_1, n_2, \dots, n_c respectively. Next, let us construct the adjacency matrix have to have block diagonal matrices N_i with size $n_i \times n_i$ corresponding to the adjacency matrix for component i as shown below:

$$\begin{bmatrix} N_1 & 0 & \cdots & 0 & 0 \\ 0 & N_2 & \cdots & 0 & 0 \\ \vdots & \vdots & \ddots & 0 & 0 \\ 0 & 0 & 0 & N_{c-1} & 0 \\ 0 & 0 & 0 & 0 & N_c \end{bmatrix}.$$

For each component, each one has an associated eigenvector of

$$\mathbb{1}_i = [0 \ \cdots \ 0 \ \underbrace{1 \ \cdots \ 1}_{n_i} \ 0 \ \cdots \ 0].$$

From (3.2.4) we know that the eigenvectors we constructed correspond to a zero eigenvalue as they correspond to each block diagonal. Since we have c block diagonals, we therefore have c linearly independent eigenvectors associated with the eigenvalues $\lambda = 0$ as desired.

Finally, we consider the backwards direction. Assume to the contrary that we do have c linearly independent eigenvectors associated with the eigenvalues $\lambda = 0$ but we only have 1 component. We are guaranteed one zero eigenvector for our graph Laplacian, which we will call v' . Because there is only one component of the graph, we know that from the proof of (3.2.3), notably (3.10), that the graph Laplacian must satisfy the relationship

$$\sum_i \sum_j A_{ij} (v_i - v_j)^2 = 0.$$

This implies that $v_i = v_j$ for all elements. This relationship must also hold for v' as well. However, this means that all the elements in v' are the same, meaning that v' is a scalar multiple of $\mathbb{1}$. This cannot be because we cannot have c linearly independent eigenvectors, contrary to our assumption. Thus

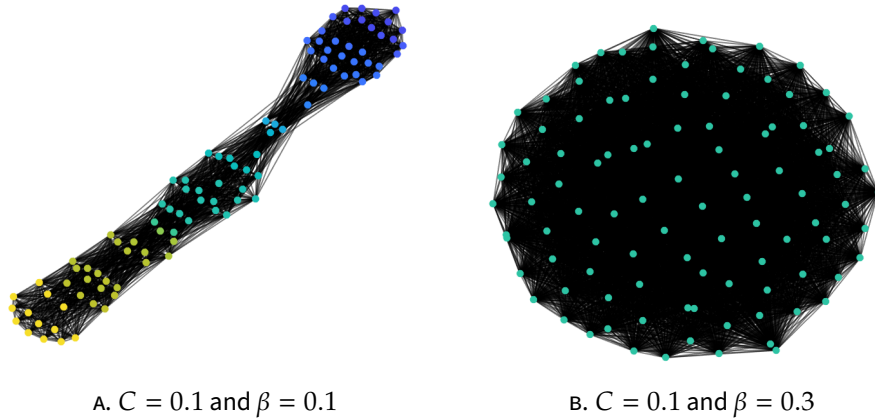


FIGURE 3.1 The converged model for $C = 0.1$ and $\beta = 0.1$ for 3.1a and $C = 0.1$ and $\beta = 0.3$ for 3.1b. Observe that the number of components would be calculated to be 1 in either case but the distribution of opinions varies widely. Notice though that if we were to use the difference metric that $d < 1$ for 3.1a while $d = 1$ for 3.1b.

it cannot be that we cannot only have 1 component. We may repeat this argument for components less than c . For components more than c , say $c + 1$, this will yield $c + 1$ zero eigenvectors, which cannot be because this implies that the geometric multiplicity is greater than algebraic multiplicity (which is false). Thus, we must have exactly c components when we have c zero eigenvectors. \square

The theorem above is profound as we may analyze the number of components of a graph simply by computing the number of zero eigenvectors of the graph Laplacian.

3.3 The Difference Metric

Early runs of the converged models suggested that the structure of converged models sometime differed in that the number of components did not align with the distribution of opinions. Consider two examples below, one where $C = 0.1$ and $\beta = 0.2$ and one where $C = 0.3$ and $\beta = 0.1$.

Using the component metric, the structure of the graph would be identified as the same because the number of components of the graph would register as 1. However, the graph topologies are widely different, as the former has an opinion distribution on containing many distinct values

from $[0, 1]$ while the latter only has an opinion distribution $x_i \approx 0.5$ for all i . The question then becomes how can we identify structures where the opinions of the converged model do not necessarily correspond to the number of components of the model. We do this by creating a new metric, called the “difference metric.” Let

$$d = \frac{\text{the number of components}}{\text{number of unique elements}(\lfloor x \rfloor)} \quad (3.13)$$

where x is the vector of opinion distributions of the converged model. The key insight is the denominator of the metric, where it measures the number of unique elements in the opinion distribution. With our converged models, there will be various opinion distributions such that they are sufficiently distinct from other opinions. We round each element in x to the nearest tenth place such that they correspond an opinion “bin” of some sort. Counting the number of unique elements of this rounded vector yields the number of unique opinions in the converged model. We note that $d = 1$ if and only if there is a one-to-one correspondence between the number of components and the number of unique elements in the graph. Consider 3.1b, with one dominant opinion and one cluster in the converged graphs. It also may suggest that if $d = 1$ and the number of clusters is greater than one, that each cluster contains a unique opinion from one another. For $d < 1$, this suggest that the number of unique elements is greater than the number of components. One example is 3.1a where we see we have one cluster but a uniform distribution of opinions throughout. This would correspond to a difference metric of $d = 0.4$.

One objection may be made is that the rounding of the number of elements may miss opinion bins if the opinions are sufficiently close. We do not have sufficient evidence to prove this, but in simulations that were run because of the averaging of the opinions if the opinions were sufficiently close to each other, we expect the opinions would converged to the average of those opinions. Notice that in the examples above that the distinct opinion clusters that formed were those whose difference were significant. Furthermore, for the purpose of analyzing our model, we simply wanted a metric to differentiate when we have one dominant cluster and one dominant opinion from other forms, indicated above. The final metric, the scalar assortativity coefficient, helps us distinguish more of the structure.

3.4 Scalar Assortativity Coefficient

Our final metric that we use to evaluate converged models is called the **scalar assortativity coefficient**, a metric of measuring how characteristics align with the connectivity of a network, as explained in Newman (2018). We say a network is assortative if the connectivity among agents correlate with the studied characteristics. The scalar assortativity coefficient is given by

$$r = \frac{\sum_{ij} A \left(A_{ij} - \frac{k_i k_j}{2m} \right) x_i x_j}{\sum_{ij} A \left(k_i \delta_{ij} - \frac{k_i k_j}{2m} \right)} \quad (3.14)$$

where x_i is the opinion of node i , A represents the adjacency matrix of the converged graph (and thus $A_{ij} = 1$ if there is an edge between node i and j and 0 otherwise), k_i is the degree of node i and m is the total number of edges in the converged graph. We note that that $r \in [-1, 1]$. What r indicates to us is if there is any correlation between the features of the graph and the connectivity via the edges in the graph. When $r = 1$, this tells us that the graph is perfectly assortative and the the opinions perfectly align up with the structure of the network. When $r = -1$, this tells us there's an inverse relationship between the opinions of the graph and the structure of the network, that is edges only occur between nodes of different opinions. When $r = 0$, this tells us that there is no correlation between the opinions of the graph and the topology of the network. One may ask how one gets this interpretation from the above formula. It may be helpful to think about the formula in terms of expectation. The term

$$A_{ij} x_i x_j$$

gives us the actual number of opinions given the adjacency matrix while

$$\frac{k_i k_j x_i x_j}{2m}$$

gives us the expected value of the degree distribution of the network. Specifically this quantity gives the expected value of the opinion distribution according to the degree distribution of the network. Thus when the expected value exactly equals that of the true network topology, it is no better than being connected randomly and thus there is no correlation between the

opinions and the network topology. We note that the denominator serves as a normalizing constant.

Chapter 4

Results of the Adaptive HK Model

4.1 Analyzing the HK model

In this section we give the analysis of the converged model. For all models given below we ran 100 trials and we averaged the summary statistics accordingly for the figures. Furthermore, the number of nodes in the model is $N = 100$. We noted that there were two significant differences when (1) updating, then rewiring versus (2) rewiring, then updating. As a result, we give the analysis for each of these results below. For each ordering, there are various initial topologies that we run the model under in order to understand the effect of initial topologies on the summary statistics.

4.2 Graph topologies of interest

The initial graph topologies of interest are: the Erdős–Rényi model, the configuration model, the complete graph, cycle, barbell, star, and square lattice. The graphs, definitions, and visual examples can be found in Table 4.1.

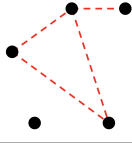
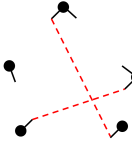
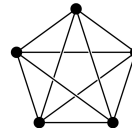
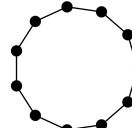
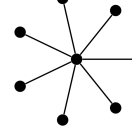
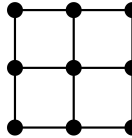
NETWORK	DEFINITION	EXAMPLE
$G(n, p)$	The Erdős–Rényi model is a random graph with two parameters, p and N , where p represents the probability there is an edge between given any two nodes among the N nodes. ¹	
C_n^λ	The configuration model is a graph that first initializes <i>stubs</i> , which are nodes that have an assigned degree drawn from a Poisson distribution. In our model, the Poisson distribution had rate $\lambda = 4$. We then iterate through each stub and assign edges to each available stub.	
K_n	A complete graph of size n is defined to be a graph where for any node they have a connection to every other node in the graph, without any self loops.	
C_n	We define a cycle of n nodes to have each node that have a degree of 2 with no self-loops.	
B_n	We define a barbell of nodes n to contain two subgraphs of $n/2$ complete graphs and one edge that connects the subgraphs together.	
S_n	We define a star of n nodes to be a 2-partite graph where the partite sets are of size 1 and $n - 1$ respectively.	
S_l	We define a square lattice based on its length $l \in \mathbb{Z}^{\geq 0}$ and we say that the number of nodes in the graph is $n = (l+1)^2$. We define a square lattice to be the graph with the node set $\{(x, y) \mid 0 \leq x, y \leq l, \text{ with } x, y \in \mathbb{Z}\}$ and edges $((x_1, y_1), (x_2, y_2))$ such that $\ (x_1 - x_2), (y_1 - y_2)\ _2 = 1$.	

TABLE 4.1 The graphs—and their corresponding definitions and examples—that we study in the model. In the network examples, the solid black lines denote deterministic edges while the red dashed lines denote probabilistic edges. Inspiration for this table was drawn from (Meng et al., 2018).

4.3 Update, then rewire

In this section, we run the version of the model where we update the opinions of the agent first, then perform the rewire step. For a recap of the overview of the algorithm, see Algorithm 1.

4.3.1 Convergence Time

The results summarizing the convergence time for various initial graph topologies can be found in Figure 4.1. We observe that there was **only** dependence on C . When $C = 0$, this results in the quickest convergence time. We believe this is the case because no opinions change in the first two time steps as $C = 0$ imposes that condition that no agents exchange opinions among each other. Because no agents exchange opinions with each other, the convergence criteria is met, resulting in a convergence time of $t = 2$. Furthermore, we note that the slowest convergence time occurs for $0.2 \lesssim C \lesssim 0.3$ —why could this be? We believe this is because we update opinions first and the confidence parameter bound of $0.2 \lesssim C \lesssim 0.3$ is big enough (but not too small!) such that the agents are receptive, not so much, that they are pulled by extremes of opinions.² Although the opinions are drawn from a uniform distribution from the interval $[0, 1]$, opinions are not established to an average of the opinions. As the model progresses, agents are being pulled fragmented opinions that slowly converge to either two dominant opinions or one dominant opinion.³

For $C \approx 0.2$ there are two dominant opinions and for $C \approx 0.3$ there is only one dominant opinion, as indicated by the difference metric of approximately 0.5 versus the one approximately 1 in Figure 4.3. For $C \gtrsim 0.3$ the convergence time speeds up because agents are less receptive and more welcoming to different opinions. This results in agents converging to the dominant average opinion of $x \approx 0.5$ and no longer changing.

²You can imagine this being analogous to a really indecisive person trying to buy ice cream and your friends are there trying to convince you to get the best ice cream. It, however, takes a long time for you guys to decide on your ice cream because you are open to ideas slightly different from yours, but your friends are so hungry that they are indecisive themselves, so your ice cream opinion changes *and* your friends' ice cream opinion changes as well, *but* not too much that you are sure what ice cream you want. The next thing you know, an hour has past, time that could have been reduced to five minutes if no one was indecisive and hungry. The moral of the story is that going to Handels with hungry friends is a bad, bad idea.

³See section 4.3.2 and 4.3.3 on the rationale of why there are one and two dominant opinions.

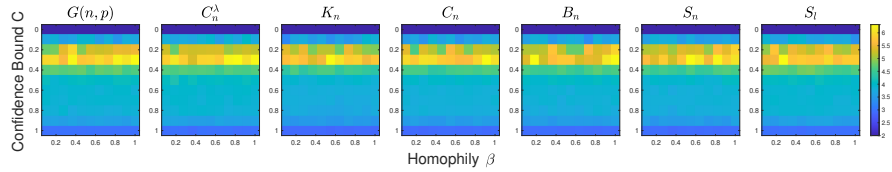


FIGURE 4.1 Convergence times for the various graph topologies for $n = 100$. The deepest shade of blue represents the fastest convergence time of $t = 2$ while the yellow represents the slowest convergence time of $t = 7$.

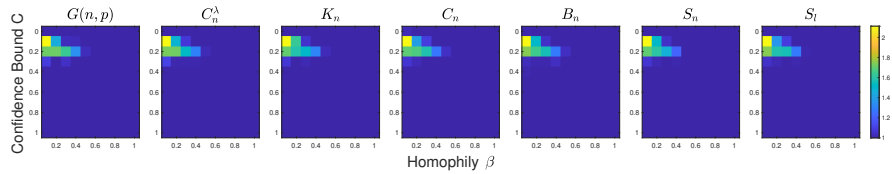


FIGURE 4.2 Number of components for the various graph topologies for $n = 100$. The deepest shade of blue represents the smallest number of components of $c = 1$ while the yellow represents the largest number of components of $c \approx 2$.

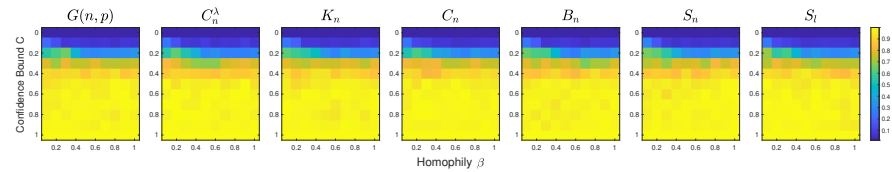


FIGURE 4.3 The difference metric for various graph topologies for $n = 100$. The deepest shade of blue represents the smallest difference metric value of $d = 0.1$ while the yellow represents the largest value of $d = 1$.

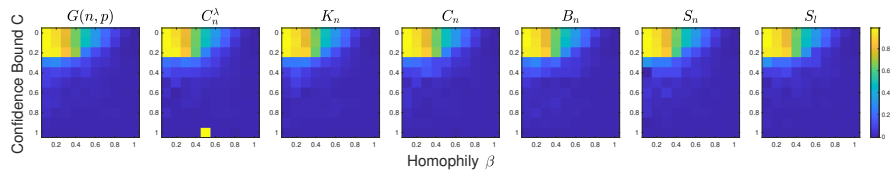


FIGURE 4.4 The scalar assortativity coefficient for $n = 100$. The deepest shade of blue represents the smallest scalar assortativity coefficient of $r = 0$ while the yellow represents the largest coefficient value of $r = 1$.

One last interesting phenomenon that occurs is when $C = 1$, where the convergence time speeds up again but not as fast as $C = 0$. This is because this $C = 1$ is the French–Degroot model and agents update opinions based only on the connectivity, not on receptivity and there is no struggle to be pulled toward an average and hence no additional time is added for this struggle.

4.3.2 Components

Convergence time, however, doesn't inform us entirely of the story behind this model. As we hinted above, there is a the emergence of dominant opinions that affects convergence time. With the addition of adaptive edges, the number of components changes—and indeed they do with a dependence on both C and β . The results summarizing the number of components can be found in Figure 4.2. We observe that the initial graph topologies do not affect the number of components when $n = 100$. We first note that for $C = 0$ that the number of components is $c = 1$ because only the rewiring step only happens and the dissolution of edges is counteracted by reestablishment of edges to like-minded agents. Because the opinions are uniformly distributed and we reestablish edges probabilistically, more often than not we get $c = 1$. We also note that the seemingly “interesting” part seems to occur when $0.1 \lesssim C \lesssim 0.2$ and $0.1 \lesssim \beta \lesssim 0.4$ —values that do not fall within these range have their 1 component at convergence. The max number of components is $c \approx 2$ for $C \approx 0.1$ and $\beta \approx 0.1$. For $C \approx 0.2$ and $0.1 \lesssim \beta \lesssim 0.3$ the number of components is $c \approx 1.7$. This suggests the emergence of two components appear more often than one component in the graphs.⁴ For $C \approx 0.1$ and $\beta \approx 0.2$ note that there are some emergence of graphs with two components, but the model is more likely to have one component. As β increases, we note that the number of components decreases because agents are less likely to exceed a bigger value of β and thus less likely to dissolve connections to form components.

4.3.3 Difference Metric

Could that be all that we can find out about the structure of the model just from the number of components and the convergence time? Surely not! Indeed, Figure 3.1 showed us that the number of components reveal one part of story but not all—namely the *distribution of opinions in a component*. The

⁴Recall that components can only be integer values.

difference metric gives us a proxy understanding of what the distribution of opinions are and the results summarizing the difference metric found in Figure 4.3. As with the prior summary statistics, we note that results stayed invariant for different initial graphs and $n = 100$ nodes. For $0 \lesssim C \lesssim 0.1$ the difference metric was $0.1 \lesssim d \lesssim 0.2$, suggesting that the converged graph maintained a distribution of approximately 10 opinion “bins” in the model. Why is this so? For $C = 0$ there are no opinions being exchanged and only the rewiring step. Because no opinions are being exchanged, the convergence criteria is met by $t = 2$ yet we maintain the uniform distribution drawn from $[0, 1]$, which sorts the opinions into 10 “bins.” What is left to consider is the component, which from 4.3.2 we know we only have 1 component for $C = 0$. This results in a difference metric of $d = \frac{1}{10} = 0.1$.

A similar phenomena occurs for $C = 0.1$. The confidence parameter is not big enough to allow for the agent’s opinions to converge quickly to a dominant opinion—rather the uniform distribution of the 10 “bins” is maintained in the cluster. As indicated by the number of components, there is a slight increase in the number of components for $\beta = 0.1$, resulting in a difference metric of approximately $d = \frac{2}{10} = 0.2$.

For $C = 0.2$ we notice that the distribution of opinions begins a phase transition. The number of components for $\beta \lesssim 0.4$ fluctuates between 1 and 2 with a difference metric of approximately 0.6. Using the difference metric formula and a value of 1.7 for the number of components, we can conclude that the average number of “bins” is approximately $\frac{1.7}{0.6} \approx 2.67$.⁵ For $\beta \gtrsim 0.4$ we note that the difference metric is $d \approx 0.3$ with one component suggests that there were 3 opinion “bins,” about the same for $\beta \lesssim 0.4$. What we notice is that the number of dominant opinions decreased and we see this trend continuing as C increases. For $C \gtrsim 0.2$ we note that we have a difference metric of $d \approx 1$ with the number of components being $c = 1$, implying that the number of opinion “bins” or dominant opinions is 1.

Thus, we conclude that as C increases that the number of “bins” or dominant opinions in the converged graph decreases. This may be explained intuitively that as agents are more receptive to different opinions that they take in different opinions that propels them to a dominant averaged opinion.

⁵We do realize that we could have calculated the number of bins directly and used that as a summary statistic itself. Hindsight is 20/20.

4.3.4 Scalar Assortativity Coefficient

The final summary statistic we explore is the scalar assortativity coefficient. The results summarizing the scalar assortativity coefficient are found in Figure 4.4. We first noticed that for $0 \lesssim C \lesssim 0.2$ that there is a dependence on β . For $\beta \lesssim 0.3$ we note that the coefficient averages to 1, indicating that graph is perfectly assortative with respect to opinions. This means that agents are connected to other agents with similar opinions. When there are more than one component, what may happen is that

1. The components either only contain a dominant opinion or
2. Agents are mostly connected to other agents with similar opinions and are sparsely connected with agents with differing opinions.

We noticed that as β increases for this C range that the coefficient decreases to 0, which may suggest that agents are no longer being connected with agents with similar opinions. An explanation for this is that for $C \lesssim 0.2$ that a uniform distribution of opinions is maintained in the network throughout and the establishment of connections via the rewiring rule connects agents with different opinions than theirs. Indeed, the number of components from Figure 4.3.2 suggests that there is only one component throughout. Furthermore, as β it becomes harder to dissolve connections, yet connections are being made.⁶ Connections are thus more likely to be maintained *and* new connections are being made as β increases. There is then an excess of edges that can result in the converged model being no better than being connected randomly as the homophily principle is exerting less force onto the model, explaining why the coefficient is decreasing.

What is perplexing is that for $C \gtrsim 0.2$ we see a coefficient of nearly 0. This seemingly contradicts with our difference metric results as they established that there was one dominant opinion in one cluster—how could it be that our model is no better than being connected randomly?

The explanation is that

1. Our rewiring rule establishes connections independent of the dissolution of edges and

⁶We note that in the rewiring rule, the dissolution of connections is independent from the establishment of edges. That is, even if there is no dissolution of edges, edges can be established. This is where our model differs from Kan et al. (2021) where their rewiring step rather has a dependency.

2. The establishment of connections has probability 1 for agents with the *exact* opinion.

1 implies that the establishment of edges always happens for each iteration, which may result in an excess of edges. Furthermore, 2 implies that if we have a component of agents with the same opinion that the component will be a complete graph. The scalar assortativity coefficient measures homophily in the sense of comparing the expected number of edges with the given characteristics with the given degree distribution to what actually occurs in the graph. When the degree distribution, however, is always that a complete graph, the expected number of edges with the characteristics will always be equivalent to a complete graph and thus these two values will be equal—resulting in a coefficient of 0. Our metric then seems contradictory because of our graphs degree distribution, but seeing this fact we realize that this is simply a shortcoming of the metric and were it not for this, the coefficient should be 1 to indicate that there is perfect assortativity occurring for $C \gtrsim 0.2$, aligning with our intuitions.⁷

4.4 Rewire, then update

In this section, we run the version of the model where we rewire first and then update the opinions of the agent. For a recap of the overview of the algorithm, see Algorithm 2.

4.4.1 Convergence Time

We begin our analysis again looking at the convergence time for various graph topologies. The results can be found in Figure 4.5. What strikes us immediately is that the convergence time is almost the same as the “Update first, then rewire” version of the model. We also note that the convergence time is constant for different initial graph topologies for $n = 100$ nodes. While there is now a dependency on both the C and β parameter, what we observe is that the slowest and fastest convergence time mirrors what we investigated in Section 4.3.2.

⁷We speculate that one may be able to revise the scalar assortativity coefficient to account for extreme cases such as this but we leave this as an exercise for the reader.

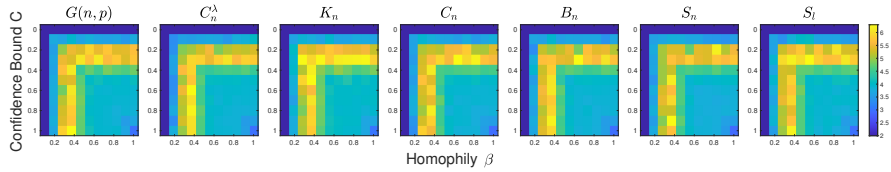


FIGURE 4.5 Convergence times for the various graph topologies for $n = 100$. The deepest shade of blue represents the fastest convergence time of $t = 2$ while the yellow represents the slowest convergence time of $t = 6$.

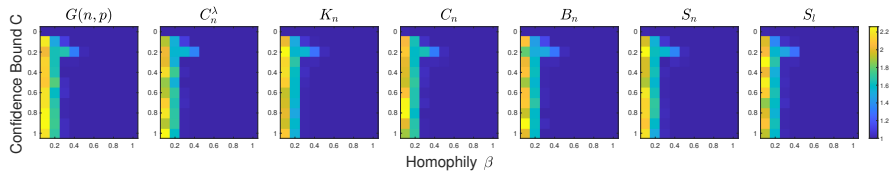


FIGURE 4.6 Number of components for the various graph topologies for $n = 100$. The deepest shade of blue represents the smallest number of components of $c = 1$ while the yellow represents the largest number of components of $c \approx 2.2$.

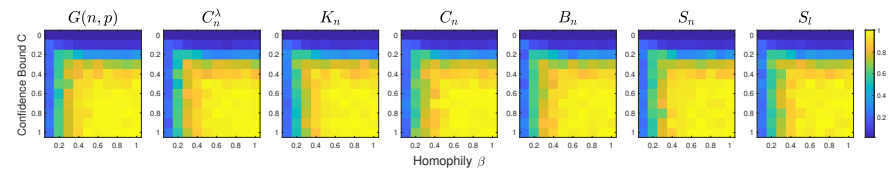


FIGURE 4.7 The difference metric for various graph topologies for $n = 100$. The deepest shade of blue represents the smallest difference metric value of $d = 0.1$ while the yellow represents the largest value of $d = 1$.

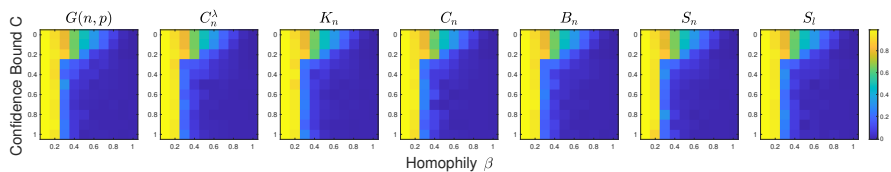


FIGURE 4.8 The scalar assortativity coefficient for $n = 100$. The deepest shade of blue represents the smallest scalar assortativity coefficient of $r = 0$ while the yellow represents the largest coefficient value of $r = 1$.

In particular, we notice that

1. the slowest convergence for $0.2 \lesssim C \lesssim 0.3$ and $0.2 \lesssim \beta \lesssim 0.3$,
2. a speed up in convergence time for $C \gtrsim 0.3$ and $\beta \gtrsim 0.3$, and finally
3. one final increase in convergence time for $C = \beta = 1$.

There is thus a symmetric phenomenon occurring here—if we we to take the upper half⁸ and reflect it across the diagonal line $C = \beta$, we would get the results in Figure 4.5. Why could this be?

Unfortunately, analysis with merely the convergence time is not sufficient to explain the phenomena occurring here. Rather, supplementary information from Sections 4.4.2, 4.4.3 and 4.4.4 is needed and we resume analysis of the convergence time in Section 4.4.5.

4.4.2 Components

Left unsatisfied by the lack of explanation of the convergence time, we look for the number of components to see what can potentially illuminate this puzzle. What immediately strikes us from the results of the number components from Figure 4.6 is that there is a column of components where $c > 1$. Indeed, for $\beta \lesssim 0.2$ and $C \gtrsim 1$ we observe that the average number of components is $c > 1$. More specifically for $\beta \approx 0.1$, we see that the number of components is $c \approx 2$ while for $\beta \approx 0.2$ the number of components is $c \approx 1.6$. We ask again, why could this be?

One thing to consider is that because we rewire first, we dissolve connections that satisfy $|x_i - x_j| > \beta$. With $0.1 \lesssim \beta \lesssim 0.2$ this is fairly easy to meet. We are left with components with agents that have opinions satisfying $|x_i - x_j| \lesssim 0.1$ or $|x_i - x_j| \lesssim 0.2$ depending on our value of β . We then reestablish connections agents probabilistically, with a greater chance of having a connection with agents whose opinions are similar to their own. What manifests are components or loosely connected communities that have very similar opinions. When we update the opinions, we note that opinions were going to be exchanged will have done so regardless of connections that would be dissolved. Furthermore, the addition of edges with like-minded agents accelerates and encourages formation of components of similar opinions that are not connected with other components. If we look

⁸Or lower half if one prefers.

at Figure 4.8 at the scalar assortativity coefficient, we see that the coefficient suggests connections of perfect assortativity, suggesting that agents are connected to agents with similar opinions to their own. We note that the number of components decreases for $\beta \approx 0.2$ because less components will form as it is harder to satisfy $|x_i - x_j| > 0.2$ than $|x_i - x_j| > 0.1$.

We note that it was interesting that for $\beta \gtrsim 0.3$ that the number of components averaged to $c = 1$, with the exception of $C \approx 0.2$. More specifically, there is a recurrence of the number of components in Section 4.3.2 of the “Update, then rewire” version for when we have $C \approx 0.2$ and $\beta \lesssim 0.4$. Because $\beta \lesssim 0.2$ has been considered, we would like to consider $0.2 \lesssim \beta \lesssim 0.4$. However, this is analogous to the case of where $\beta > C$. There are two cases that are fundamental, we (1) rewire or (2) we don’t rewire. When we do rewire, then $|x_i - x_j| > \beta$. Because we know that $\beta > C$, this implies that $|x_i - x_j| > C$ and that we do not dissolve update opinions. However, the dissolving of connections is equivalent to not updating an opinion—when connections are dissolved, they are turned “off” and the dissolving acts as a phantom confidence bound in the sense of not allowing agents to exchange opinions by virtue of the lack of connection between agents.⁹ Thus, if we are to dissolve a connection, it substitutes the opinion update in the sense that it prevents an update. If we are to not to dissolve, then the opinion update happens normally.

In both cases, the opinion update occurs and acts synonymous as if the “Update, then rewiring” step was occurring. Thus, this may explain why we see approximately the same behavior of clusters for $C = 2$ and $\beta \lesssim 0.4$.

4.4.3 Difference Metric

Once more, we investigate the distribution of opinions in the converged model via the difference metric. The results can be found in Figure 4.7 for various graph topologies. We note that for $\beta \lesssim 0.2$ that the difference metric of $r \approx 0.5$ conveys this iteration of the model has components that contain a mixture of opinions distributed throughout. From our investigation of components we note that we have more than one component for $\beta \lesssim 0.2$, barring $C = 0$. We can then expect some components that have a mixture of opinions and some subgraphs that have only one opinion in the component. For $\beta \gtrsim 0.2$ and $C \gtrsim 0.2$ we see a difference metric of $r \approx 1$. We also note

⁹The reestablishment of connections is the caveat here but we realize that if we did dissolve and the connection was indeed reestablished, the condition of $|x_i - x_j| > C$ prevents the update of the opinion again.

that the number of components from Figure 4.6 suggest for this region we have one component with one dominant opinion. For $C \lesssim 0.2$ we note that with one component throughout, we can expect a distribution of 10 “bins” throughout the component.

The behavior of the difference metric is very similar to the “Update, then rewire” version—what sets them apart is the fact that this version of the model rewires first, and thus affects the behavior for $\beta \lesssim 0.2$, creating the characteristic column we see.

4.4.4 Scalar Assortativity Coefficient

The theme of augmenting the results from the previous version of the model continues with scalar assortativity coefficient. Indeed, looking at Figure 4.8 we see that the behavior is similar to that of Figure 4.4. For $0 \lesssim C \lesssim 0.2$ we note again the eventual decrease of the coefficient, explained by the increased connectivity because of the rewiring aspect. For $\beta \lesssim 0.2$ we see the emergence of the small fragmented components emerge and, as mentioned previously, they tend to be connected with like-minded agents, but loosely enough to allow for a mixture of opinions. For $\beta \gtrsim 0.2$ and $C \gtrsim 0.3$ we note the shortcomings of the scalar assortativity coefficient once more—as the difference metric, as explained in Section 4.4.3 and seen in Figure 4.7, demonstrates that there is one component throughout with one dominant opinion. Thus, we can expect that the model has a complete graph for these parameters.

4.4.5 Convergence Time (continued)

We resume again with our analysis of the convergence time, noting that the observed characteristics of

1. the slowest convergence for $0.2 \lesssim C \lesssim 0.3$ and $0.2 \lesssim \beta \lesssim 0.3$,
2. a speed up in convergence time for $C \gtrsim 0.3$ and $\beta \gtrsim 0.3$, and finally
3. one final increase in convergence time for $C = \beta = 1$

can be explained by the fact that this version is an augmentation of the previous model with a special behavior on $\beta \lesssim 0.2$. The two thing we would like to highlight is that for $\beta = 0$ that we have a convergence time of 2, which is rather quick. The explanation we have is that $\beta = 0$ dissolves **all** connections and hence no opinions are updated.

4.5 Varying the number of nodes

In the previous sections, we noticed that the number initial graph topologies seemed to not impact the summary statistics. A question then arises: what other features of networks can we investigate? One answer is the number of nodes. We run both versions of the model on the Erdős–Rényi model with a fixed $p = 0.6$ but varying the number of nodes, which we do for $n = 10, 50, 100, 200$, and 500 . Results for the “Update, then rewire” version can be found in Figure 4.9 while the “Rewire, then update” version can be found in Figure 4.10—they are rather exciting.

4.5.1 Convergence Time

For the “Update, then rewire” version, we find that as the number of nodes increase, the region in which we see the slowest convergence time changes. We see that for $n = 10, 50$, and 100 that the slowest convergence time when $0.2 \lesssim C \lesssim 0.4$. For $n = 200$ we see that this pattern persists but we faintly see a region from $0.4 \lesssim C \lesssim 0.9$ where the convergence time slows down. For $n = 500$, we see that the $0.2 \lesssim C \lesssim 0.4$ no longer has the slowest convergence time but rather the region $0.4 \lesssim C \lesssim 0.9$ does. We also note that the colorbar tells us that the convergence time speeds up as n increases, with the average convergence time around 3.5 for $n = 500$ compared to slowest convergence time of 5 for $n = 10$.

The “Rewire, then update” version also has the same behavior as the previous version. Indeed, we see that the emergence of the $0.2 \lesssim C \lesssim 0.4$ and $0.2 \lesssim \beta \lesssim 0.4$ for $n = 100$ that contains the slowest convergence time changes to be $C, \beta \gtrsim 0.4$ when $n = 500$. Furthermore, we also note that the convergence time also speeds up as n increases as well.

4.5.2 Number of Components

The region in which we see components whose averages are greater than one remains approximately the same. Indeed, for the “Update, then rewire” version we see $c > 1$ for $C \approx 0.2$ and $\beta \lesssim 0.4$; for the “Rewire, then update” version we see $c > 1$ for $C \approx 0.2$ and $\beta \lesssim 0.2$. The noteworthy phenomenon is that as n increases, the number of components decrease regardless of the rewiring rule. Indeed, for $n = 500$ we see $c \approx 1.05$ for both versions. With the convergence time, we can speculate that the large single component forms faster as the number of nodes increases.

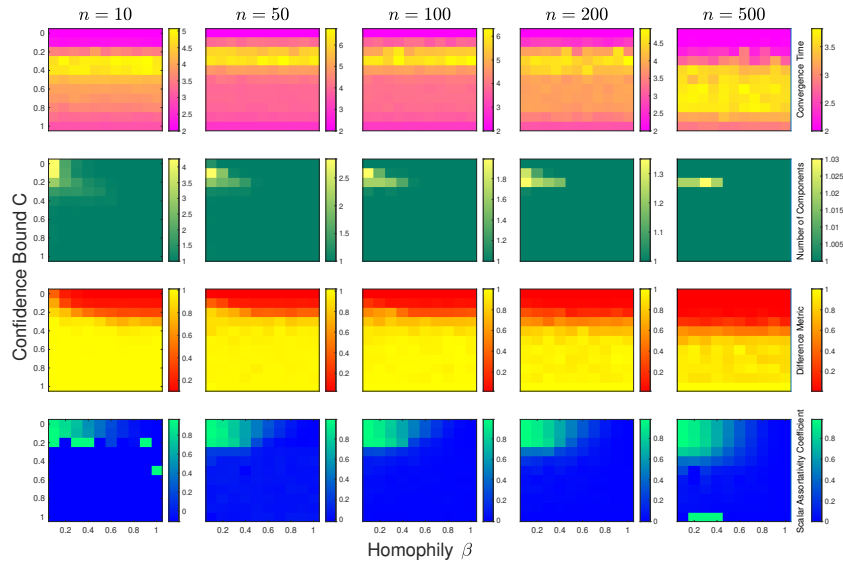


FIGURE 4.9 Summary statistics for "Update, then rewire" version on $G(n, p = 0.6)$ for various values of n .

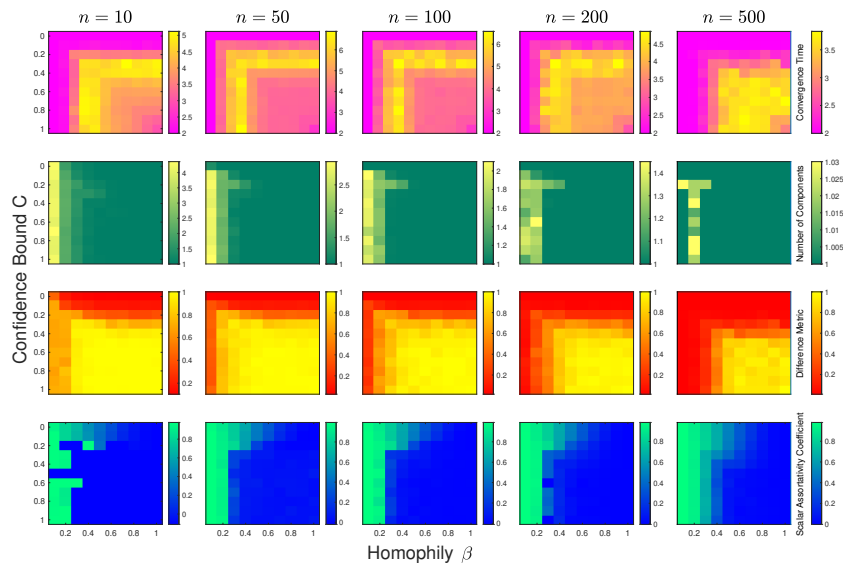


FIGURE 4.10 Summary statistics for "Rewire, then update" version on $G(n, p = 0.6)$ for various values of n .

4.5.3 Difference Metric

From the number of components, we note that are more likely to have one component as n increases. That, however, doesn't tell us the distribution of opinions in the overall graph itself. Looking at the third row for both version of the models, we find that the distribution of opinions increase. Indeed, for $n = 10$, we see primarily a difference metric of $d \approx 1$. However, for $n = 200$ and $n = 500$ we see the region for having 10 "bins" increase. For the "Update, then rewire" version, we notice this region is $C \gtrsim 0.4$ while for the "Rewire, then update" version, we notice that this region is $C, \beta \gtrsim 0.4$. Since we know that for $n = 500$ we often have one component in the converged model, this indicates that the distribution of the opinions is affected by the parameters. For the "Update, then rewire" version, since the model is only dependent on C , we note that for $C \lesssim 0.4$ we one big component but can expect almost a uniform distribution of opinions in the component. For the "Rewire, then update" version, we note that for $C, \beta \lesssim 0.4$ we can expect one large component but one dominant opinion throughout.

4.5.4 Scalar Assortativity Coefficient

Finally, the scalar assortativity coefficient can illuminate more of our puzzle. Immediately looking at the $C \gtrsim 0.4$ and $C, \beta \gtrsim 0.4$ region for the "Update, then rewire" and "Rewire, then update" version respectively, we see that we have a coefficient of $r \approx 0$. Our analysis previously tells us this is not a suggestion that the converged model is not assortative with respect to the opinions but rather these regions likely have a complete graph structure because of a shortcoming of the coefficient. For $\beta \lesssim 0.2$ for both version of the models, we see that the coefficient is $r \approx 1$, suggesting that the converged models are not as fully connected compared to a complete graph and displays perfectly assortative behavior.

4.6 Varying p in the Erdős–Rényi model

In this section, we considered what would happen if p varied for a fixed $n = 100$, and thus changing the initial connectivity among agents. $p = 0$ represents a graph that has no connections while $p = 1$ represents a complete graph. The results for the "Update, then rewire" can be found in Figure 4.11 while the "Rewire, then update" can be found in Figure 4.12. The results, to put it bluntly, are unremarkable.

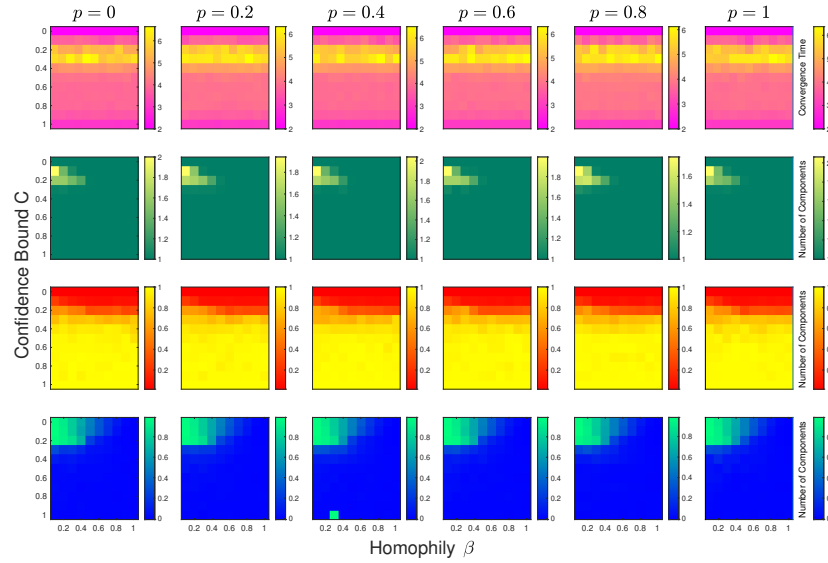


FIGURE 4.11 Summary statistics for “Update, then rewire” version on $G(n = 100, p)$ for various values of p .

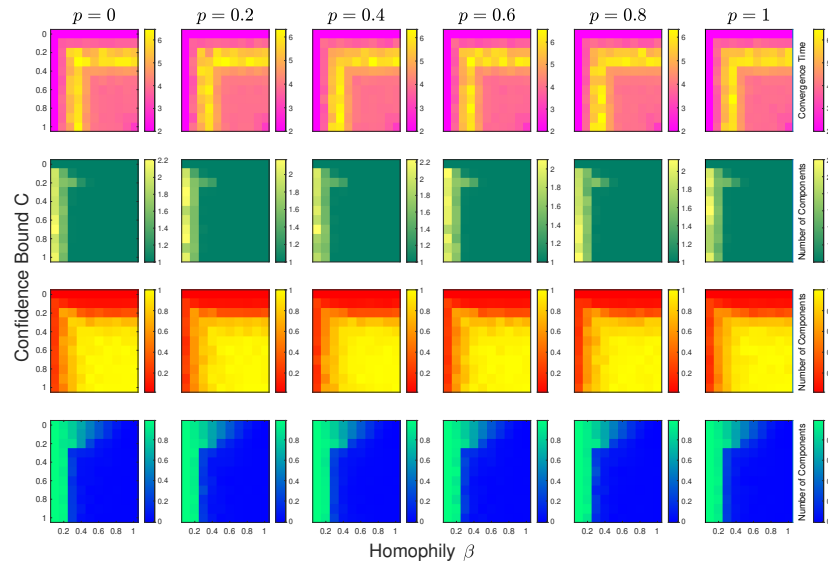


FIGURE 4.12 Summary statistics for “Rewire, then update” version on $G(n = 100, p)$ for various values of p .

As we investigated with previous graph topologies, we noted that there were no changes in quantitative behavior for the summary statistics in our results as well. Indeed, looking at all the rows at each summary statistic, we see no major changes in behavior, barring differences noise via the probabilistic aspect of establishing connections. We thus conclude that varying p and the initial graph topology has no major impact on the summary statistics and the model itself.

Chapter 5

Conclusion & Future Work

“All good things must come to an end.”

5.1 Conclusion

Many things were learned from this thesis. We learned about various models of opinion dynamics: the French–Degroot model, the Hegselmann–Krause model, the Deffaut–Weisbuch model, and an adaptive Deffaut–Weisbuch model from Kan et al. (2021). We took inspiration from Kan et al. (2021)’s work and developed an adaptive Hegselmann–Krause model, using summary statistics to understand the behavior of the model. We also further developed two versions of the model, finding the importance of the order in updating opinions and rewiring connections. In particular, our results are as follows:

For the **update, then rewire** version of the model for fixed $n = 100$ we found that

- (a) The slowest convergence time when $0.2 \lesssim C \lesssim 0.4$. When $C = 0$ we see the quickest convergence time of $t = 2$. When $C = 1$ we see the convergence time speed up, but not as quick as when $C = 0$.
- (b) The number of components was mostly $c = 1$. We found the average number of components to be $c > 1$ when $0.1 \lesssim C \lesssim 0.2$ and $C \lesssim 0.4$. The max average number of components was $c \approx 2$.

- (c) The difference metric was $d \approx 0$ for $C \lesssim 0.2$, which indicates that the distribution of opinions was similar to that of the initial distribution of opinions. For $C \gtrsim 0.2$ the difference metric was $d \approx 1$, indicating that we had a one-to-one ratio with the number of components and the number of dominant opinions. With the component information, we can conclude that it was likely that we have one large component with one dominant opinion.
- (d) The scalar assortativity coefficient shows us that for $C \lesssim 0.2$ that there was less assortative behavior with respect to agents' opinions as β increases. For $C \gtrsim 0.2$ we note that the coefficient of $r \approx 0$ conveys that there is no assortativity happens but our difference metric tells us otherwise. What is happening here is the emergence of complete graph for the large component, which predicts $r \approx 0$. This extreme cases tells us that the coefficient has a shortcoming when it comes to complete graphs.

For the **rewire, then update** version of the model for fixed $n = 100$ we found that the results were analogous to what happened in the **update, then rewire** case, but there was a particular phenomena for $\beta \lesssim 0.2$. Because we rewire first, the initial graph is fragmented and agents are likely to be rewired to agents that share similar opinions with their own, creating components of similar opinions. These characteristics manifest in the summary statistics and can be thought as augmented to the results for the **update, then rewire** version.

Next, we noted that there was a significant behavioral change when the number of nodes changes. In particular, as n increases the general structure of the converged graph tended to a single component, whose opinion distribution varied depending on the version of the model and the parameters C and β . Finally, simulations on the Erdős–Rényi graph reaffirmed the fact that the initial graph topology seemingly did not play a huge rule for the summary statistics for the fixed $n = 100$.

5.2 Future Work

Our work hopefully illuminates exciting inquires one can take up. With our findings we found shortcomings as well. As mentioned in (d), we found the scalar assortativity coefficient's limit when exposed to a complete graph with similar characteristics throughout—rather than indicating a perfectly

assortative graph it indicates a graph that was no better than connected randomly with respect to the opinions. Indeed, this was based on the calculation of comparing the expected edges with the opinions with respect to the degree distribution and to the actual connectivity with the opinions. Some future work may include accounting for this extreme and developing a new version of the coefficient.

Further potential future work may include expanding upon the proposed model or changing the assumptions with it. Our work was based on the social phenomenon of homophily but other rewiring rules modeling other social phenomena, such as replicating the mechanism of retweeting on Twitter, could be explored. Furthermore, our rewiring rule did not separate the dissolving of edges with the reestablishment of edges—rather they were independent. This feature explained the phenomenon of the complete graph component with one dominant opinion throughout. Work can be done to have the rewiring rule have the two aspects be augmented with one another.

One may also explore a different convergence criteria for this model as well. Recall that we said our model converged if the difference between the opinion in the prior time step did not change significantly, given by $\varepsilon = 10^{-4}$. For an adaptive model, however, it may be desirable instead to impose a convergence criteria based on the connections—that is let the model converge in the connections among agents.

After further developing and studying this model more in-depth, one could also extend this model to include Zinn-Brooks and Porter's work on studying media influence in online social networks (Brooks and Porter, 2020). In particular, we are excited to consider time-evolving edges and see how our model predicts polarization and connections between these polarized communities. We also would like to further develop this model to be a multi-layer graph with time dependent connections (Kivela et al., 2014). In particular, it would be interesting to consider one layer representing social media interactions and one layer representing real world interactions.

Bibliography

Baumann, Fabian, Philipp Lorenz-Spreen, Igor M. Sokolov, and Michele Starnini. 2020. Modeling Echo Chambers and Polarization Dynamics in Social Networks. *Physical Review Letters* 124(4):048,301. doi:10.1103/PhysRevLett.124.048301.

Brooks, Heather Z., and Mason A. Porter. 2020. A model for the influence of media on the ideology of content in online social networks. *Physical Review Research* 2(2):023,041. doi:10.1103/PhysRevResearch.2.023041.

Cinelli, Matteo, Emanuele Brugnoni, Ana Lucia Schmidt, Fabiana Zollo, Walter Quattrociocchi, and Antonio Scala. 2020. Selective Exposure shapes the Facebook News Diet. <https://arxiv.org/abs/1903.00699>.

Degroot, Morris H. 1974. Reaching a Consensus. *Journal of the American Statistical Association* 69(345):118–121. doi:10.1080/01621459.1974.10480137.

Del Vicario, Michela, Gianna Vivaldo, Alessandro Bessi, Fabiana Zollo, Antonio Scala, Guido Caldarelli, and Walter Quattrociocchi. 2016. Echo Chambers: Emotional Contagion and Group Polarization on Facebook. *Scientific Reports* 6(1):37,825. doi:10.1038/srep37825.

Dewey, John. 1927. *The Public and Its Problems*. Holt Publishers.

Flaxman, Seth, Sharad Goel, and Justin M. Rao. 2016. Filter Bubbles, Echo Chambers, and Online News Consumption. *Public Opinion Quarterly* 80(S1):298–320. doi:10.1093/poq/nfw006.

Hegselmann, Rainer, and Ulrich Krause. 2002. Opinion Dynamics and Bounded Confidence Models, Analysis, and Simulation. *Journal of Artificial Societies and Social Simulation* 5(3):33.

- . 2015. Opinion dynamics under the influence of radical groups, charismatic leaders, and other constant signals: A simple unifying model. *Networks & Heterogeneous Media* 10(3):477. doi:10.3934/nhm.2015.10.477.
- Kan, Unchitta, Michelle Feng, and Mason A. Porter. 2021. An adaptive bounded-confidence model of opinion dynamics on networks. doi:10.48550/ARXIV.2112.05856. URL <https://arxiv.org/abs/2112.05856>.
- Kivela, M., A. Arenas, M. Barthelemy, J. P. Gleeson, Y. Moreno, and M. A. Porter. 2014. Multilayer networks. *Journal of Complex Networks* 2(3):203–271. doi:10.1093/comnet/cnu016. URL <https://doi.org/10.1093%2Fcomnet%2Fcnu016>.
- Lawler, Gregory F. 2010. *Random Walk and the Heat Equation*. No. v. 55 in Student Mathematical Library, Providence, R.I: American Mathematical Society.
- Lippmann, Walter. 1922. *Public Opinion*. Harcourt, Brace & Co.
- Liu, Qiming, Tao Li, and Meici Sun. 2017. The analysis of an SEIR rumor propagation model on heterogeneous network. *Physica A: Statistical Mechanics and its Applications* 469:372–380. doi:10.1016/j.physa.2016.11.067.
- Mann, Thomas E., and Norman J. Ornstein. 2012. *It's Even Worse Than It Looks: How the American Constitutional System Collided With the New Politics of Extremism*. Basic Books.
- McPherson, Miller, Lynn Smith-Lovin, and James M Cook. 2001. Birds of a Feather: Homophily in Social Networks. *Annual Review of Sociology* 27(1):415–444. doi:10.1146/annurev.soc.27.1.415.
- Meng, X. Flora, Robert A. Van Gorder, and Mason A. Porter. 2018. Opinion Formation and Distribution in a Bounded Confidence Model on Various Networks. *Physical Review E* 97(2):022,312. doi:10.1103/PhysRevE.97.022312. 1701.02070.
- Newman, M. E. J. 2018. *Networks*. Oxford Univeristy Press, Oxford, UK, second edition.
- Sloss, David L. 2020. Information Warfare and Democratic Decay. SSRN Scholarly Paper ID 3743824, Social Science Research Network, Rochester, NY. doi:10.2139/ssrn.3743824.

Wang, Jiajia, Lijun Zhao, and Rongbing Huang. 2014. SIRaRu rumor spreading model in complex networks. *Physica A: Statistical Mechanics and its Applications* 398:43–55. doi:10.1016/j.physa.2013.12.004.

Whipple, Mark. 2005. The Dewey-Lippmann Debate Today: Communication Distortions, Reflective Agency, and Participatory Democracy. *Sociological Theory* 23(2):156–178. doi:10.1111/j.0735-2751.2005.00248.x.